Chinese Journal of Polymer Science Vol. 35, No. 3, (2017), 422–433

Chinese Journal of Polymer Science
© Chinese Chemical Society
Institute of Chemistry, CAS
Springer-Verlag Berlin Heidelberg 2017

Fabrication of Polythiophene Patterns through Blending of a Thermally Curable Polythiophene with Poly(methyl methacrylate) and Selective Thermal Curation*

Mushtaque A. Memon[a, b], Jin-hua Sun[b], Hee-Tae Jung[c**], Shou-ke Yan[a**] and Jian-xin Geng[b**]

[a] *State Key Laboratory of Chemical Resource Engineering, Beijing University of Chemical Technology, Beijing 100029, China*

[b] *Technical Institute of Physics and Chemistry, Chinese Academy of Sciences, Beijing 100190, China*

[c] *National Research Laboratory, Department of Chemical and Biomolecular Engineering (BK-21), Korea Advanced Institute of Science and Technology, 373-1 Guseong-dong, Yuseong-gu, Daejeon 305-701, Korea*

Abstract In this study, we demonstrate a novel method for fabricating polythiophene patterns, *i.e.*, cylindrical holes and cylinders, through blending of a thermally curable polythiophene carrying with tertiary ester groups (PT-*tert*-ESTER) and poly(methyl methacrylate) (PMMA), followed by thermal conversion of the PT-*tert*-ESTER to an insoluble polythiophene *via* low-temperature cleavage of the tertiary ester groups and removal of the PMMA component *via* ultraviolet degradation. We show that the surface polarity of substrates, the mass ratio of PT-*tert*-ESTER to PMMA in the blend solutions as well as the concentration of the blend solutions strongly influence the formation of the polythiophene patterns. Cylindrical holes are more readily formed on less polar substrates when a PT-*tert*-ESTER dominated blend solution is used, while cylinders are more readily formed on more polar substrates when a PMMA dominated blend solution is used. Moreover, the diameters of both the cylindrical holes and the cylinders decrease as the PT-*tert*-ESTER concentration is increased in the respective ranges of the PT-*tert*-ESTER/PMMA ratios where the patterns are formed. Grazing incident X-ray diffraction data have indicated that the patterning of the PT-*tert*-ESTER component in the blend films improves the crystallinity of PT-*tert*-ESTER as well as the molecular packing of the insoluble polythiophene in the resultant patterned polythiophene films.

Keywords Polythiophene; Patterns; Cylindrical holes; Cylinders; Blending

Electronic Supplementary Material Supplementary material is available in the online version of this article at http://dx.doi.org/10.1007/s10118-017-1895-8.

INTRODUCTION

Conjugated polymers such as polythiophene, polypyrrole, polyacetylene, and poly(*para*-phenylene vinylene) have attracted considerable attention in recent years due to their potential applications in polymer-based electronics and optoelectronics such as light-emitting diodes[1–6], field-effect transistors[7–10], photovoltaic

* This work was financially supported by the National Natural Science Foundation of China (Nos. 21274158 and 91333114), the National Research Laboratory Program of the Korea Science and Engineering Foundation (KOSEF), the World Class University Program (No. R32-2008-000-10142-0), and the Center for Nanoscale Mechatronics & Manufacturing (08K140100414, CNMM).

** Corresponding authors: Hee-Tae Jung, E-mail: heetae@kaist.ac.kr
Shou-ke Yan (闫寿科), E-mail: skyan@mail.buct.edu.cn
Jian-xin Geng (耿建新), E-mail: jianxingeng@mail.ipc.ac.cn

Received September 20, 2016; Revised October 11, 2016; Accepted October 24, 2016
doi: 10.1007/s10118-017-1895-8

devices[11–16], sensors[17–24], and energy storage[25, 26]. In the aforementioned applications, control of the morphology and structure of conjugated polymer films is prerequisite for enhancing their optoelectronic properties[14, 27, 28]. In particular, patterned conjugated polymers films have been intensively investigated for the application in polymer-based electronic and optoelectronic devices because the composite films with optimized surface morphologies produce highly ordered and well-defined donor-acceptor interfaces, in which the charge trapping at the bottlenecks in randomly distributed bulk heterojunction films is avoided, as a result, leading to enhanced device performance[29–31].

To date, patterned conjugated polymer films have been primarily obtained by several approaches: (1) micro-phase separation in diblock copolymer films, followed by selective removal of one component in the films[32, 33], (2) micro-phase separation in polymer blend films coated on patterned substrates, in which the patterned underlying surfaces are designed to preferentially interact with one component in the blends[34–36], (3) surface-initiated polymerization on patterned substrates[37, 38], and (4) soft lithography technique[39, 40]. However, each of the aforementioned approaches suffers different disadvantages to a certain extent. For example, the micro-phase separation in diblock copolymer films suffers poor reproducibility and tedious thermal annealing during preparation; the substrate pattern induced micro-phase separation in polymer blend films requires a complicated fabrication of substrate patterns.

Herein, we propose a simple and reproducible method, which utilized the micro-phase separation between a soluble polythiophene carrying with tertiary ester (PT-*tert*-ESTER) and poly(methyl methacrylate) (PMMA), thermal curation of the PT-*tert*-ESTER fraction, and degradation and removal of the PMMA fraction by ultraviolet (UV) irradiation, for preparing polythiophene films with cylindrical holes or cylinders. PT-*tert*-ESTER was used in this study because it is soluble in common solvents and capable of conversion into its polythiophene counterpart *via* thermal cleavage of the tertiary ester groups. We show that the patterns of the polythiophene films were strongly affected by the surface polarity of the substrates, the concentration of the blend solutions, and the mass ratio between PT-*tert*-ESTER to PMMA. The polythiophene patterns, *i.e.*, cylindrical holes and cylinders, prepared in this study show advantages in high reproducibility and large-area preparation. The impact of the patterning of PT-*tert*-ESTER in the blend films on its crystalline structures and on the molecular packing of the resultant insoluble polythiophene was investigated using grazing incidence X-ray diffraction (GIXRD). The methodology developed may provide a new approach for controlling the morphologies of conjugated polymer films for the applications in electronics and optoelectronics.

EXPERIMENTAL

Materials

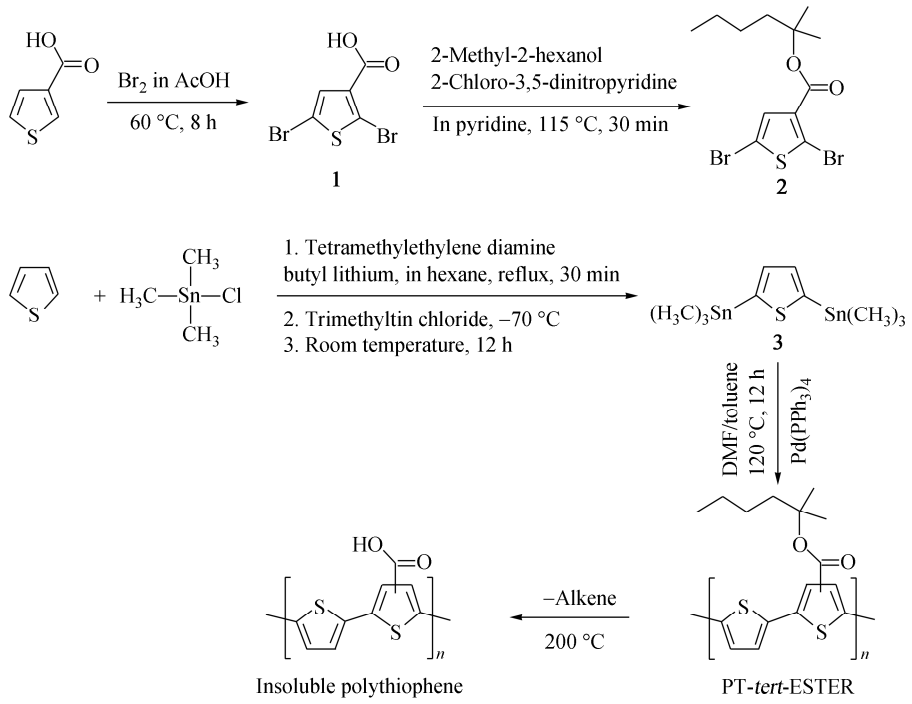
Scheme 1 illustrates the synthetic route of poly(3-(2-methyl-2-hexylcarboxylate)thiophene-*co*-thiophene) (PT-*tert*-ESTER) through a Stille coupling reaction from 2-methyl-2-hexyl-2,5-dibromothiophene-3-carboxylate (**2**) and 2,5-bis-trimethylstannanylthiophene (**3**) according to previous reports[41, 42]. The PT-*tert*-ESTER can be converted to an insoluble polythiophene by thermal annealing at *ca*. 200 °C *via* cleavage of the tertiary ester groups. PMMA (M_w = 15000 by GPC) used in this study was purchased from Aldrich.

Preparation of Polythiophene Patterns

Indium tin oxide (ITO) coated glass slides were cleaned by sequential sonication in each of the following solvents (*i.e.*, chloroform, acetone, deionized water, and isopropyl alcohol) for 15 min, followed by oxygen plasma treatment. In this study, three types of surfaces, *i.e.*, oxygen plasma-treated ITO surfaces, poly(3,4-ethylenedioxythiophene)-poly(styrenesulphonate) (PEDOT:PSS) surfaces, and the insoluble polythiophene surfaces, were used. PEDOT:PSS surfaces were obtained by spin-coating a layer of PEDOT:PSS on the oxygen plasma-treated ITO substrates. Insoluble polythiophene surfaces were obtained by thermal annealing of the PT-*tert*-ESTER layers spin-coated on PEDOT:PSS surfaces.

In Scheme 2 the overall procedure for preparing polythiophene hole structures on the PEDOT:PSS surface is illustrated. In detail, a PEDOT:PSS layer with approximately 30 nm was first spin-coated on an oxygen

plasma-cleaned ITO substrate, and thermally annealed at 200 °C for 5 min (Scheme 2a). Then, a PT-*tert*-ESTER/PMMA layer was spin-coated using a PT-*tert*-ESTER/PMMA blend solution in chlorobenzene. Phase separation between PT-*tert*-ESTER and PMMA took place during solvent evaporation (Scheme 2b). After fully dried, the PT-*tert*-ESTER/PMMA film was subjected to thermal annealing at 200 °C for 20 min to convert PT-*tert*-ESTER to the insoluble polythiophene (Scheme 2c). Polythiophene hole structures were finally obtained by UV irradiation (40 min) to selectively degrade the PMMA component and removal of degraded products through sonication (5 min) in acetic acid (Scheme 2d).

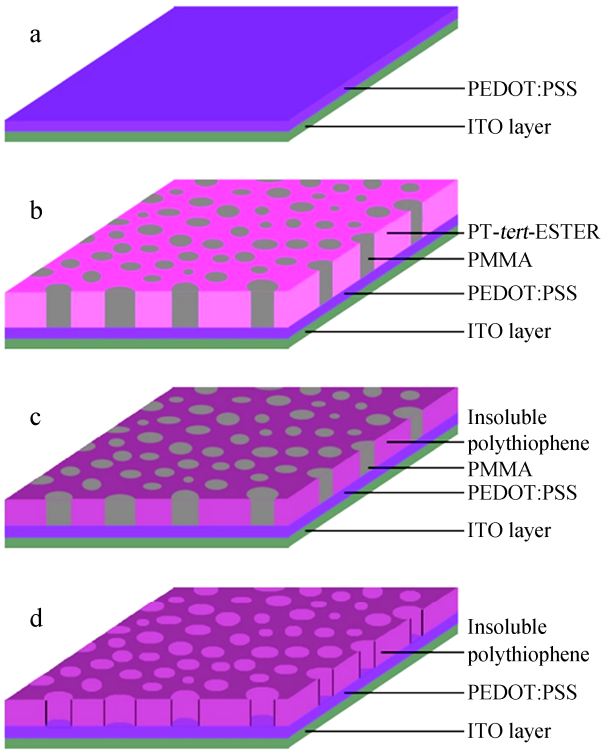


Scheme 1 Synthesis of PT-*tert*-ESTER and conversion of PT-*tert*-ESTER to an insoluble polythiophene

Polythiophene cylinder structures were prepared by following a similar procedure, in which more polar surfaces (*i.e.*, oxygen plasma-treated ITO surfaces and insoluble polythiophene surfaces) as well as PMMA component dominated PT-*tert*-ESTER/PMMA blend solutions were used.

Characterization

The molecular weight and polydispersity index of PT-*tert*-ESTER were determined using gel permeation chromatography (GPC, a GPC 515-2410 system) using polystyrene standard in THF. Thermal stability of the PT-*tert*-ESTER was investigated using a differential scanning calorimeter (DSC 204 F1 Phoenix) and thermogravimetric analyzer (TG 209 F3) under an atmosphere of N_2 at a scanning rate of 5 $K \cdot min^{-1}$. FTIR spectra were recorded on a JASCO FT/IR-470 Plus spectrometer using polymer films coated on silicon wafers. A Bruker AMX500 NMR (500 MHz), using TMS ($\delta = 0$) or the residual proton resonance of deuterated $CDCl_3$ ($\delta = 7.26$) as the internal standard, was used to characterize the molecular structures during synthesis of PT-*tert*-ESTER. Atomic force microscopy (AFM) images were obtained on an SPA 3800N microscope with a SPA-400 scanner. Two-dimensional GIXRD images were obtained using a high-power X-ray beam from a synchrotron radiation source (4C2 beamline, Pohang Accelerator Laboratory, South Korea) and a detection system equipped with a two-dimensional X-ray detector (PI-SCX4300-165/2, Princeton Instrument). The wavelength of the X-ray was 0.13807 nm and the incident angle was fixed at 0.2°.



Scheme 2 A scheme for preparation of cylindrical holes in polythiophene films

RESULTS AND DISCUSSION

PT-*tert*-ESTER was polymerized through a Stille coupling reaction (Scheme 1). The weight-averaged molecular weight of PT-*tert*-ESTER was measured to be 4.76×10^4 with a polydispersity index of 2.28 using GPC with polystyrene standard in THF. Thermal analysis showed that the PT-*tert*-ESTER underwent an endothermal reaction at *ca*. 200 °C, accompanied with *ca*. 21% mass loss (Fig. S1 in supporting information, SI). This reaction corresponded to the conversion of PT-*tert*-ESTER to the insoluble polythiophene due to thermal cleavage of the *tert*-ester groups (Scheme 1). The thermal conversion of PT-*tert*-ESTER to the insoluble polythiophene was also confirmed using FTIR spectroscopy (Fig. S2 in SI).

Figure 1(a) shows an AFM image of a PT-*tert*-ESTER/PMMA blend film coated on the PEDOT:PSS surface using a blend solution in chlorobenzene with a PT-*tert*-ESTER concentration of 15 mg·mL^{-1} and a PT-*tert*-ESTER/PMMA mass ratio of 8:2. The film exhibited a morphology containing phase-separated domains with lateral dimensions of *ca*. 2 μm and *ca*. 150 nm. In thin films composed of two polymers, the film morphologies formed during spin-coating are necessarily influenced by both the miscibility between the two polymers as well as the surface energy of the substrate. A basic condition for two polymers to mix is that the Gibbs free energy of the mixture must be less than the sum of the Gibbs free energies of the individual components, *i.e.*, $\Delta G_{mix} = \Delta H_{mix} - T \cdot \Delta S_{mix} < 0$, where the ΔG_{mix} stands for the increase in free energy on mixing, ΔH_{mix} is the enthalpy of mixing, and ΔS_{mix} is the entropy of mixing[43]. The phase separation for immiscible polymers is a thermodynamic process; namely, given enough time to separate, the immiscible polymer blend will demix and form separate phases with minimal area of interfaces. However, the thermodynamic equilibrium is hard to obtain because spin-coating method turns out to be a solvent quenching process: the solvent evaporates quickly during the spin-coating of a homogeneous solution. In this process, the preferential interaction of the underlying substrate with one of the two polymers induces the phase separation to take place in a specific way. It was already reported that a normal or lateral organization of the phase-separated domains is governed by a complex interplay between the preferential aggregation of one phase on the substrate and the phase separation in

the film[44–46]. Therefore, the phase-separated domains in the AFM image of the PT-*tert*-ESTER/PMMA blend film (Fig. 1a) were attributed to the compromise between the thermodynamic driving force for phase separation and the kinetic process of polymer aggregation, which was slow due to the rapid increase of solution's viscosity during quick solvent evaporation.

Figure 1(b) shows that the *ca*. 2 μm domains protruded and the *ca*. 150 nm domains became unnoticeable after the PT-*tert*-ESTER/PMMA film was thermally annealed at 200 °C for 20 min, because of the shrinkage of the PT-*tert*-ESTER component upon its conversion to the insoluble polythiophene. Thickness measurement indicated that the PT-*tert*-ESTER films decreased by 52% in thickness due to the cleavage of the *tert*-ester groups. The polythiophene hole structures were finally obtained after the PMMA component was degraded by irradiation of UV light and was removed by washing with acetic acid (Fig. 1c). Thus, it was clearly verified that the separated domains with sizes of both *ca*. 2 μm and *ca*. 150 nm corresponded to PMMA phase (Fig. 1a). The protruding feature of the PT-*tert*-ESTER phase (Fig. 1a), confirmed by its brighter contrast than that of the PMMA phase, was likely due to the different solubilities of the two polymers in the common solvent[46], chlorobenzene in this study. In the process of spin-coating, PT-*tert*-ESTER, which has lower solubility, solidified first and formed edges at the interfaces between the PT-*tert*-ESTER and the PMMA domains, whereas the PMMA, which has higher solubility, resided between the edges. With evaporating solvent, PMMA finally solidified with more shrinkage because it was more swollen with the solvent than PT-*tert*-ESTER. Therefore, the PMMA phase was found to be sunken in the PT-*tert*-ESTER/PMMA blend film (Fig. 1a). The smaller holes could be attributed to the smaller domains of PMMA that were formed by deep quenching during rapid solvent evaporation[46].

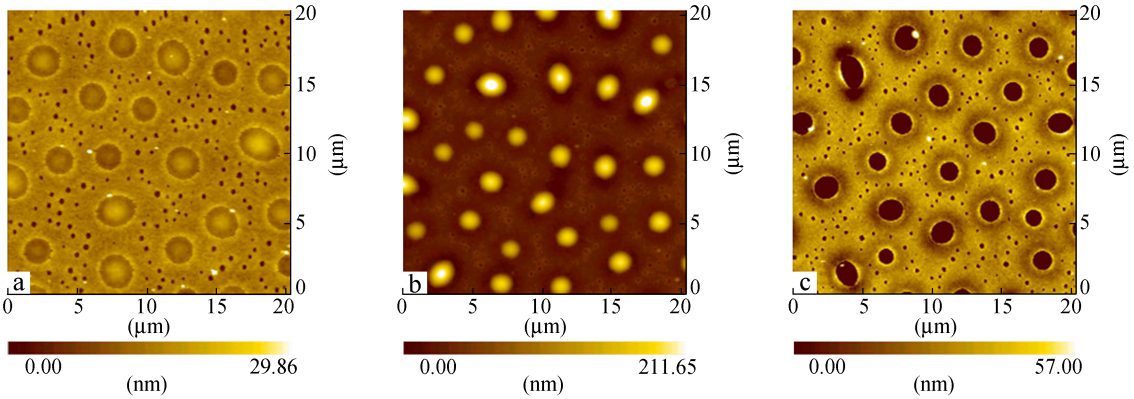


Fig. 1 AFM images of (a) a PT-*tert*-ESTER/PMMA blend film spin-coated on the PEDOT:PSS surface, (b) the polythiophene/PMMA film obtained after the film shown in panel (a) was thermally annealed at 200 °C for 20 min, (c) the hole-patterned polythiophene film obtained after the film shown in panel (b) was irradiated with UV light and washed with acetic acid

We found that the morphologies of the PT-*tert*-ESTER/PMMA films coated on the PEDOT:PSS surfaces were strongly influenced by the mass ratio of the two components in the blend solutions (Fig. 2). AFM observation indicates that the influence of PT-*tert*-ESTER/PMMA ratio on polythiophene morphology can be divided into three regions: the ratio is smaller than 1:8, between 2:8 and 8:8, and greater than 8:4. When the PT-*tert*-ESTER/PMMA ratio was smaller than 1:8, polythiophene cylinder structures were obtained (Fig. 2a), indicating that the PT-*tert*-ESTER phase existed in a form of cylinders in the blend film. Careful observation revealed that the edges of the cylinders' top were sharp (Fig. 2a), because of the first solidification of the PT-*tert*-ESTER phase to form edges upon solvent evaporation in the process of film formation[46]. When the PT-*tert*-ESTER/PMMA ratio fell between 2:8 and 8:8 (Figs. 2b–2d), the morphology of the polythiophene films became featureless except for loop-shaped edges protruding out of the films, which was also attributed to the first solidification of the PT-*tert*-ESTER phase during the early stage of solvent evaporation. Finally, when the PT-

tert-ESTER/PMMA ratio was greater than 8:4 (Figs. 2e–2h), hole structures vertical to the substrates were found in the polythiophene films. And the diameter of the cylindrical holes decreased with increasing the concentration of the PT-*tert*-ESTER component in the blend solutions. Cross section analysis of the AFM images indicated that the cylindrical holes in the polythiophene films obtained from a PT-*tert*-ESTER/PMMA blend solution with the component ratio of 8:2 had a depth that was equal to the thickness of the polythiophene films. This finding indicated that the cylindrical holes in the polythiophene films were penetrated to the substrate surface.

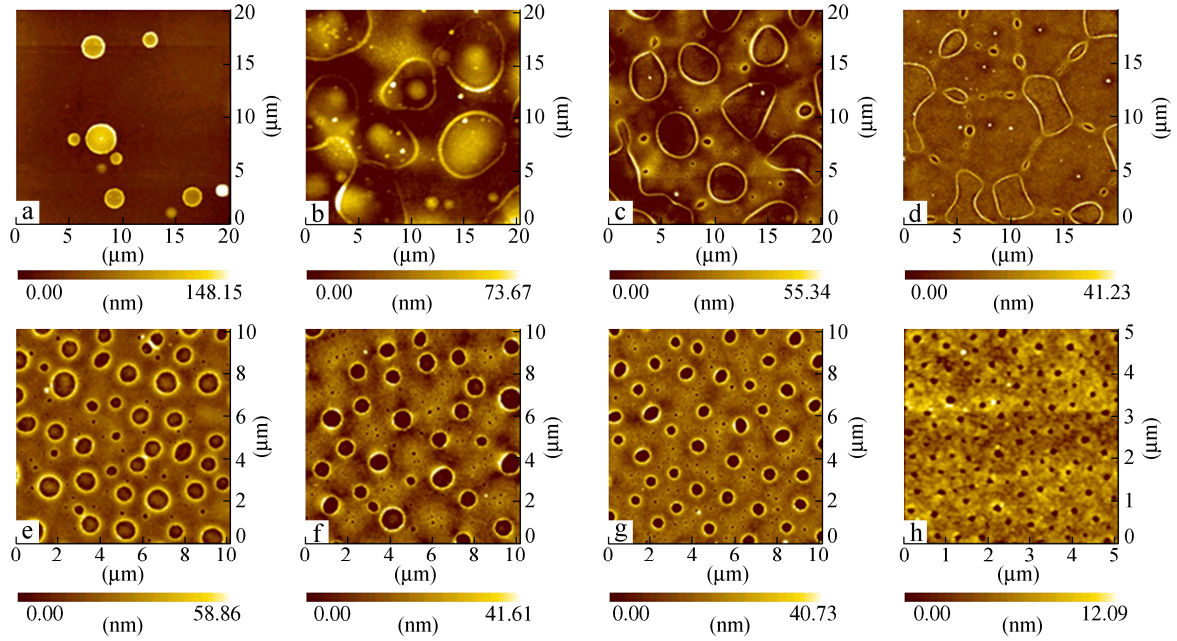
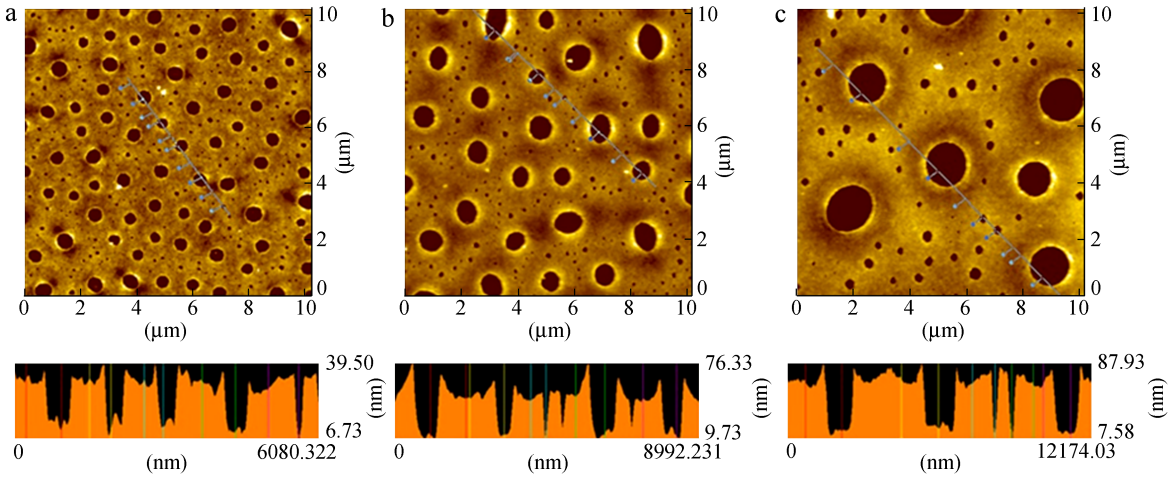


Fig. 2 AFM images of the polythiophene structutres formed on the PEDOT:PSS surfaces as the function of PT-*tert*-ESTER/PMMA ratio: (a) 1:8, (b) 2:8, (c) 4:8, (d) 8:8, (e) 8:4, (f) 8:3, (g) 8:2, and (h) 8:1 (The blend solutions had a constant PT-*tert*-ESTER concentration of 11 mg·mL^{-1}.)

Additionally, we found that the diameter of cylindrical holes could also be adjusted by varying the concentration of the PT-*tert*-ESTER/PMMA blend solution. It was found that the diameter of the polythiophene holes prepared on the PEDOT:PSS surfaces increased as the concentration of the PT-*tert*-ESTER/PMMA blend solution increased (Fig. 3). The measurement based on approximately 100 holes revealed that a PT-*tert*-ESTER/PMMA blend solution with PT-*tert*-ESTER concentration of 10 mg·mL^{-1} produced cylindrical holes with diameters of *ca.* 442 and 82 nm, while *ca.* 770 and 110 nm cylindrical holes were obtained for a blend solution with the PT-*tert*-ESTER concentration of 15 mg·mL^{-1} as well as *ca.* 1480 and 150 nm cylindrical holes obtained for a blend solution with the PT-*tert*-ESTER concentration of 20 mg·mL^{-1}. As we discussed above, the formation of the PMMA micro-domains in the PT-*tert*-ESTER/PMMA blend films, which finally resulted in cylindrical holes after the PMMA fraction was removed, was basically a phase separation process during solvent evaporation. Therefore, the rapid solvent evaporation was likely to "freeze" the highly dispersed state of the PMMA micro-domains in the PT-*tert*-ESTER matrix to obtain small holes. Obviously, at the initial stage of the spin-coating, a higher concentration solution produced a thicker wet film that contained a larger quantity of solvent, resulting in a longer time for the solvent to evaporate; therefore, during the elongated period of solvent evaporation for the higher concentration solution, smaller PMMA domains in the wet film were likely to coalesce. As a result, the PT-*tert*-ESTER/PMMA blend solution with the higher concentration produced larger cylindrical holes (Fig. 3c). Moreover, the depth of the cylindrical holes was also found to increase as the concentration of the PT-*tert*-ESTER/PMMA blend solution increased: *i.e.*, *ca.* 22 nm depth for a blend solution

with the PT-*tert*-ESTER concentration of 10 mg·mL^{-1}, *ca*. 33 nm depth for a blend solution with the PT-*tert*-ESTER concentration of 15 mg·mL^{-1}, and *ca*. 53 nm depth for a blend solution with PT-*tert*-ESTER concentration of 20 mg·mL^{-1}.



	*Z*1 (nm)	*Z*2 (nm)	Δ*Z* (nm)
	33.2	11.2	21.9
	33.0	11.3	21.7
	33.2	12.5	20.6
	32.1	10.3	21.7
	28.5	6.73	21.8

	*Z*1 (nm)	*Z*2 (nm)	Δ*Z* (nm)
	13.6	46.0	32.4
	45.6	13.5	32.1
	43.7	10.9	32.7
	46.7	14.3	32.4
	45.6	13.0	32.6

	*Z*1 (nm)	*Z*2 (nm)	Δ*Z* (nm)
	69.3	16.9	52.3
	71.4	18.8	52.6
	65.9	13.6	52.2
	14.2	66.1	51.9
	65.6	13.4	52.1

Fig. 3 The polythiophene cylindrical holes prepared from PT-*tert*-ESTER/PMMA solutions with various PT-*tert*-ESTER concentrations: (a) 10 mg·mL^{-1}, (b) 15 mg·mL^{-1}, and (c) 20 mg·mL^{-1}
The blend solutions had a constant PT-*tert*-ESTER/PMMA ratio of 8:2. In the cross section analysis, *Z*1 and *Z*2 represent the relative heights of the indicated points on the cross-section lines and Δ*Z* represents the depths of the correspondding holes.

Moreover, the polythiophene patterns were also strongly influenced by the surface properties of the substrates. In Fig. 4(a) the diagrams of the polythiophene patterns formed on three different surfaces are summarized, *i.e.*, the PEDOT:PSS surfaces (Fig. 4a1), the oxygen plasma-treated ITO surfaces (Fig. 4a2), and the insoluble polythiophene surfaces (Fig. 4a3), as function of the PT-*tert*-ESTER/PMMA ratio. Clearly, the oxygen plasma-treated ITO surfaces had higher surface polarity than the PEDOT:PSS surfaces due to the introduction of polar groups on ITO surfaces during oxygen plasma treatment, so did the insoluble polythiophene surfaces due to the presence of the carboxylic acid groups attached to polythiophene backbones. The cylindrical hole structures were more readily formed on less polar surfaces, *i.e.*, the PEDOT:PSS surfaces. By contrast, the cylinder structures were more readily formed on more polar surfaces, *i.e.*, the oxygen plasma-treated ITO surfaces and the insoluble polythiophene surfaces. Figures 4(b) and 4(c) show the AFM images of typical polythiophene cylinders prepared on the insoluble polythiophene surfaces using a blend solution with the PT-*tert*-ESTER/PMMA ratio of 3:8. Carrying with the ester groups, the PT-*tert*-ESTER has lower polarity than the insoluble polythiophene; and therefore, it must show less compatibility with the more polar surfaces, *i.e.*, the oxygen plasma-treated ITO surfaces and the insoluble polythiophene surfaces, than with the less polar surface, *i.e.*, the PEDOT:PSS surfaces. As a result, the PT-*tert*-ESTER component was likely to form a minimum interface area with the insoluble polythiophene substrates, resulting in the formation of cylinders vertical to the substrates. In addition, the polythiophene cylinders formed on the oxygen plasma-treated ITO surfaces and the insoluble polythiophene surfaces had cleaner background, with no featureless polythiophene domains remained. By contrast, featureless polythiophene domains, coexisting with polythiophene cylinders, were readily found on the PEDOT:PSS surface, indicating better compatibility of PT-*tert*-ESTER with the PEDOT:PSS surface. These

findings further confirmed that the more polar surfaces with less compatibility with the PT-*tert*-ESTER phase facilitated the formation of cylindrical structures; meanwhile, the less polar surfaces that show more compatibility with the PT-*tert*-ESTER phase facilitated the formation of hole structures.

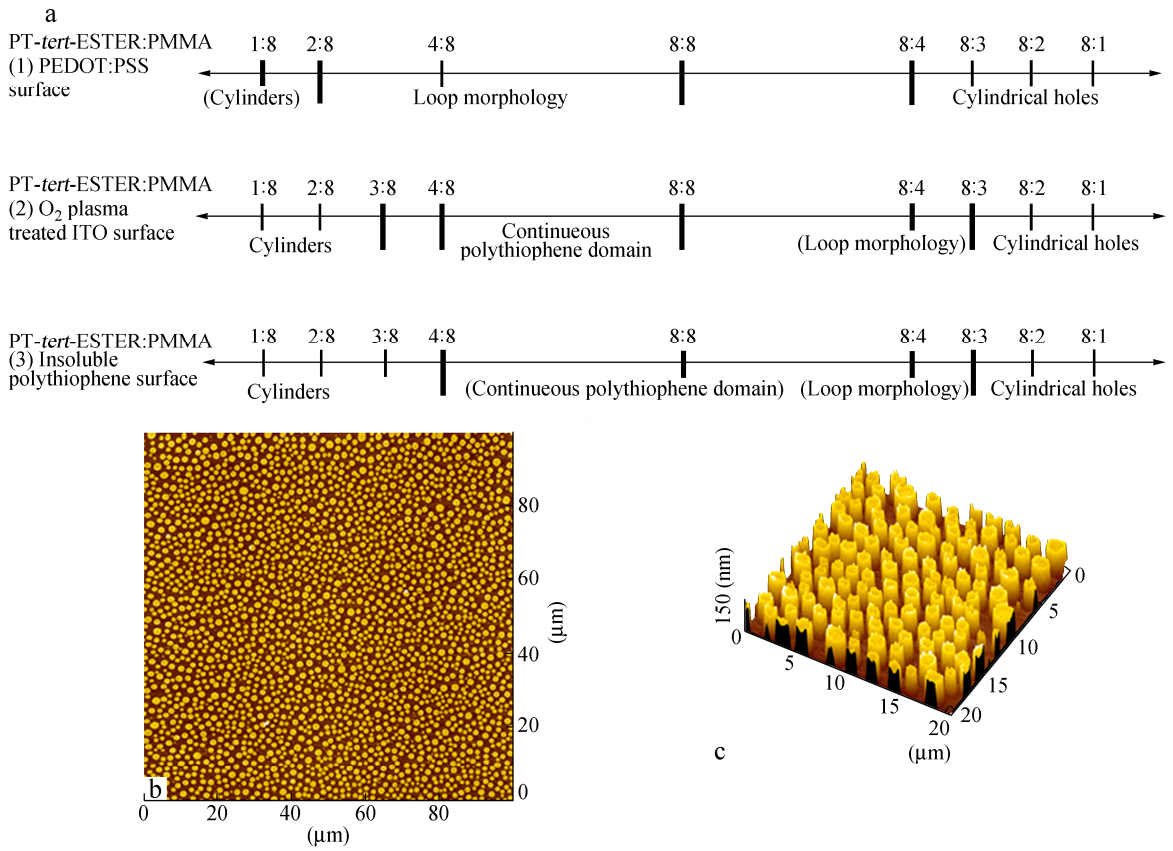


Fig. 4 (a) The diagrams of the polythiophene patterns formed on the surfaces of the PEDOT:PSS, the surfaces of the oxygen plasma-cleaned ITO, and the surfaces of the insoluble polythiophene (All the bars on the concentration axes represent the mass ratios tested; the long bold bars represent the mass ratios from which the films start to exhibit the designated patterns; the short bold bars represent the mass ratios at which the films exhibit the designated structures.); (b) Typical cylinders formed on the surface of the insoluble polythiophene using a blend solution with the PT-*tert*-ESTER/PMMA ratio of 3:8 and PT-*tert*-ESTER concentration of 11 mg·mL^{-1}; (c) The magnified three dimensional image of the cylinders

Similar to the influence of the PT-*tert*-ESTER/PMMA ratio on the diameter of the cylindrical holes (Figs. 2f–2h), the cylinders were also impacted by the component ratio of the blend solutions. Figure 5 shows the AFM images of the polythiophene cylinders formed on the insoluble polythiophene surfaces: the diameter of the cylinders decreased with increasing PT-*tert*-ESTER/PMMA ratio in the blend solutions. Additionally, the cylinders formed with a PT-*tert*-ESTER/PMMA ratio of 3:8 exhibited more uniform diameter than those formed with component ratios of 2:8 and 1:8. Although the cylinders provided limited spaces for the crystallization of PT-*tert*-ESTER, the dimensions of the cylinders are larger than the size of the polythiophene crystal whiskers reported[47]. Therefore, the PT-*tert*-ESTER may crystallize in the same way in the cylinder domains as it does in thin films.

In order to investigate the evolution of the crystalline structures during the conversion of the PT-*tert*-ESTER to the insoluble polythiophene and the impact of the patterns on molecular orientation in the films, GIXRD characterization was performed using the pristine PT-*tert*-ESTER films and the PT-*tert*-ESTER/PMMA

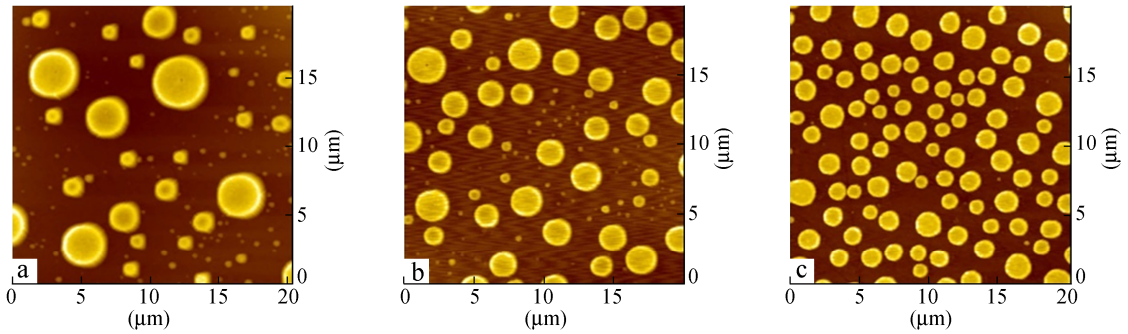


Fig. 5 AFM images of the polythiophene cylinders prepared on the surfaces of the insoluble polythiophene using PT-*tert*-ESTER/PMMA blend solutions with various component ratios: (a) 1:8, (b) 2:8 and (c) 3:8 (The blend solutions had a constant PT-*tert*-ESTER concentration of 11 mg·mL^{-1}.)

blend films. Figure 6(a) illustrates the setup for GIXRD measurements of thin film samples to obtain crystalline information in the out-of-plane direction, in which GIXRD patterns were recorded by a two-dimensional detector. Incidence of X-ray with a grazing angle ensures a maximum pathway for the X-ray passing through thin film samples, providing stronger diffraction patterns[48]. Figures 6(d)–6(f) display the GIXRD patterns of a pristine PT-*tert*-ESTER film, the PT-*tert*-ESTER film thermally annealed at 150 °C, and the insoluble polythiophene film that was obtained by thermally annealing a PT-*tert*-ESTER film at 200 °C. The PT-*tert*-ESTER film exhibited a two-dimensional pattern containing (100) and (020) arcs (Fig. 6d), with these two diffractions deriving from different crystalline domains. The indexing of the PT-*tert*-ESTER GIXRD pattern was done by referring the well-studied poly(3-alkylthiophene)[49]. Upon annealing at 150 °C, the (100) and (200) diffraction arcs became more intense (Fig. 6e), with disappearance of the (020) arcs, indicating that molecular rearrangement had taken place during thermal annealing, leading to improved molecular orientation of the PT-*tert*-ESTER with the side-chain groups vertical to the substrate (Fig. 6b). However, with entire disappearance of the (100) and (200) diffraction arcs, the GIXRD pattern recorded for the insoluble polythiophene film contained a relatively stronger (020) diffraction arc compared to the patterns recorded for the PT-*tert*-ESTER film (Fig. 6f versus 6e and 6d). This finding indicated that molecular rearrangement had occurred in the films during the thermal conversion of PT-*tert*-ESTER to the insoluble polythiophene, leading to dominated orientation of the main-chains of the insoluble polythiophene parallel to the substrate (Fig. 6c). Figures 6(g)–6(i) display the GIXRD patterns of the PT-*tert*-ESTER/PMMA blend film (8:2 in mass ratio), the PT-*tert*-ESTER/PMMA blend film thermally annealed at 150 °C, and the resultant insoluble polythiophene film with hole structures. The PT-*tert*-ESTER in the as-prepared PT-*tert*-ESTER/PMMA blend film as well as the insoluble polythiophene in the hole-patterned polythiophene film respectively provided more intense diffraction arcs than they did in the corresponding pristine films (Fig. 6g versus 6d, Fig. 6i versus 6f and Fig. S3 in SI). Thermal annealing led to similarly intensified (100) and (200) diffractions in the PT-*tert*-ESTER film and the PT-*tert*-ESTER/PMMA blend film (Fig. 6e versus 6h and Fig. S3 in SI). These findings implied that the PT-*tert*-ESTER had higher crystallinity in the as-prepared PT-*tert*-ESTER/PMMA blend films than in its pristine films, and that the insoluble polythiophene had higher crystallinity in the hole-patterned film than in the continuous film. Such results should be related to the formation of the hole structures. As we discussed above, the hole structures were formed by first solidification of the PT-*tert*-ESTER at the interfaces between PT-*tert*-ESTER and PMMA. Therefore, the vertical interfaces between PT-*tert*-ESTER and PMMA were likely responsible for the higher crystallinity and enhanced molecular orientation for the PT-*tert*-ESTER in the PT-*tert*-ESTER/PMMA blend film and, thereafter, the insoluble polythiophene in the hole-patterned polythiophene film. The electronic properties of conjugated polymers are basically related to their crystalline structures[14, 50, 51]. Therefore, the patterning of polythiophene films may provide a potential approach for improving their electronic properties.

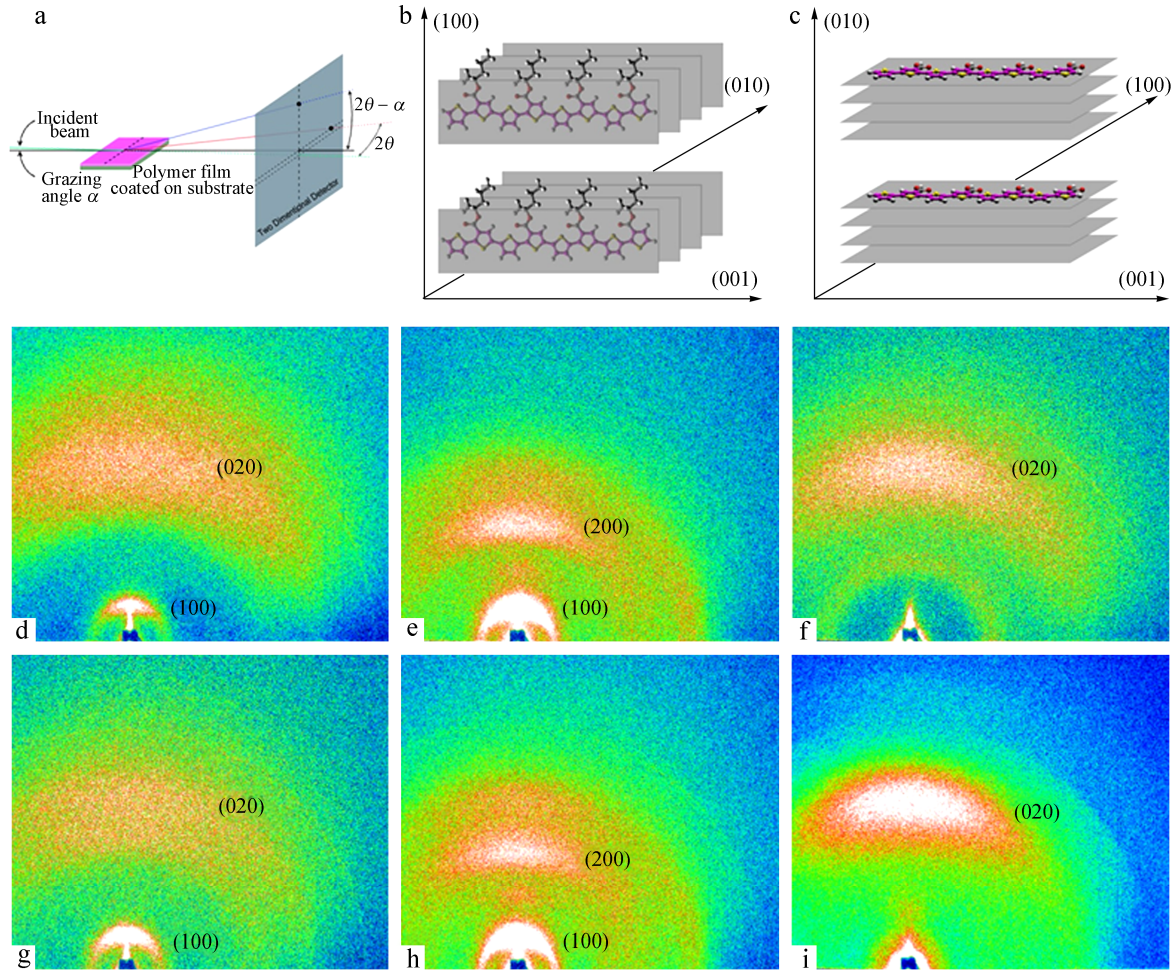


Fig. 6 (a) The experimental setup for GIXRD characterization of thin films; (b) An illustration showing that the side-chain groups of the PT-*tert*-ESTER are vertical to the substrate; (c) An illustration showing that the main-chains of the insoluble polythiophene are parallel to the substrate; (d–i) Two-dimensional GIXRD patterns of (d) the as-prepared PT-*tert*-ESTER film coated on the PEDOT:PSS surface, (e) the PT-*tert*-ESTER film annealed at 150 °C for 15 min, (f) the insoluble polythiophene film obtained by annealing the PT-*tert*-ESTER film at 200 °C for 20 min, (g) the as-prepared PT-*tert*-ESTER/PMMA film coated on the PEDOT:PSS surface, (h) the PT-*tert*-ESTER/PMMA film annealed at 150 °C for 15 min and (i) the hole patterned polythiophene film obtained by annealing the PT-*tert*-ESTER/PMMA film at 200 °C for 15 min and removal of the PMMA component

CONCLUSIONS

Polythiophene films with patterns of vertical cylindrical holes or cylinders have been prepared by a successive procedure consisting of blending of the PT-*tert*-ESTER and PMMA, thermal curation of the PT-*tert*-ESTER, and removal of the PMMA component *via* UV degradation. The morphologies of the blend films are strongly influenced by the concentration of the PT-*tert*-ESTER/PMMA blend solution, the component ratio, and the substrate properties. Vertical cylindrical hole structures are more readily formed on a less polar substrate such as the PEDOT:PSS surfaces using the PT-*tert*-ESTER component dominated blend solutions. On the other hand, vertical cylinder structures are more readily formed on more polar substrates such as the oxygen plasma-treated ITO surfaces and the insoluble polythiophene film surfaces using the PMMA component dominated blend solutions. GIXRD data have indicated that the patterning of the PT-*tert*-ESTER component in the blend films improves the crystallinity of PT-*tert*-ESTER as well as the molecular packing of the insoluble polythiophene in

the resultant patterned polythiophene films. We expect that these patterns will open up new applications for conjugated polymers in techniques such as light-emitting diodes, photovoltaic devices, and sensors.

REFERENCES

1 Lam, J.W.Y. and Tang, B.Z., Acc. Chem. Res., 2005, 38(9): 745
2 Lee, T.W., Adv. Funct. Mater., 2007, 17(16): 3128
3 Lee, T.W., Chung, Y., Kwon, O. and Park, J.J., Adv. Funct. Mater., 2007, 17(3): 390
4 Dyreklev, P., Berggren, M., Inganas, O., Andersson, M.R., Wennerstrom, O. and Hjertberg, T., Adv. Mater., 1995, 7(1): 43
5 Goh, C., Kline, R.J., McGehee, M.D., Kadnikova, E.N. and Frechet, J.M.J., Appl. Phys. Lett., 2005, 86(12): 122110
6 Braun, D., Gustafsson, G., McBranch, D. and Heeger, A.J., J. Appl. Phys., 1992, 72(2): 564
7 Yang, H.C., Shin, T.J., Yang, L., Cho, K., Ryu, C.Y. and Bao, Z.N., Adv. Funct. Mater., 2005, 15(4): 671
8 Ong, B.S., Wu, Y.L., Liu, P. and Gardner, S., Adv. Mater., 2005, 17(9): 1141
9 McCulloch, I., Bailey, C., Giles, M., Heeney, M., Love, I., Shkunov, M., Sparrowe, D. and Tierney, S., Chem. Mater., 2005, 17(6): 1381
10 Park, Y.D., Kim, D.H., Lim, J.A., Cho, J.H., Jang, Y., Lee, W.R., Park, J.H. and Cho, K., J. Phys. Chem. C, 2008, 112(5): 1705
11 Scharber, M.C., Wuhlbacher, D., Koppe, M., Denk, P., Waldauf, C., Heeger, A.J. and Brabec, C.L., Adv. Mater., 2006, 18(6): 789
12 Chochos, C.L., Economopoulos, S.P., Deimede, V., Gregoriou, V.G., Lloyd, M.T., Malliaras, G.G. and Kallitsis, J.K., J. Phys. Chem. C, 2007, 111(28): 10732
13 Geng, J.X., Kong, B.S., Yang, S.B., Youn, S.C., Park, S., Joo, T. and Jung, H.T., Adv. Funct. Mater., 2008, 18(18): 2659
14 Geng, J.X. and Zeng, T.Y., J. Am. Chem. Soc., 2006, 128(51): 16827
15 Qin, R.P., Jiang, Y.R., Zhang, H.X., Zhang, K.X., Zhang, Q.Y. and Chang, F.G., Chinese J. Polym. Sci., 2015, 33(3): 490
16 Keshtov, M.L., Marochkin, D.V., Fu, Y.Y., Xie, Z.Y., Geng, Y.H., Kochurov, V.S. and Khokhlov, A.R., Chinese J. Polym. Sci., 2014, 32(7): 844
17 Li, B., Sauve, G., Iovu, M.C., Jeffries-El, M., Zhang, R., Cooper, J., Santhanam, S., Schultz, L., Revelli, J.C., Kusne, A.G., Kowalewski, T., Snyder, J.L., Weiss, L.E., Fedder, G.K., McCullough, R.D. and Lambeth, D.N., Nano Lett., 2006, 6(8): 1598
18 Nilsson, K.P.R. and Inganas, O., Nat. Mater., 2003, 2(6): 419
19 Tang, Y.L., He, F., Yu, M.H., Feng, F.D., An, L.L., Sun, H., Wang, S., Li, Y.L. and Zhu, D.B., Macromol. Rapid Commun., 2006, 27(6): 389
20 Li, C., Numata, M., Takeuchi, M. and Shinkai, S., Angew. Chem., Int. Ed., 2005, 44(39): 6371
21 Meng, D., Yang, S., Sun, D., Zeng, Y., Sun, J., Li, Y., Yan, S., Huang, Y., Bielawski, C.W. and Geng, J., Chem. Sci., 2014, 5(8): 3130
22 Yang, S., Meng, D., Sun, J., Hou, W., Ding, Y., Jiang, S., Huang, Y., Huang, Y. and Geng, J., RSC Adv., 2014, 4(48): 25051
23 Yang, S., Meng, D., Sun, J., Huang, Y., Huang, Y. and Geng, J., ACS Appl. Mater. Interfaces, 2014, 6(10): 7686
24 Zhang, H., Zhang, G., Xu, J.K., Wen, Y.P., Ding, W.C., Zhang, J., Ming, S.L. and Zhen, S.J., Chinese. J. Polym. Sci., 2016, 34(2): 229
25 Memon, M.A., Bai, W., Sun, J.H., Imran, M., Phulpoto, S.N., Yan, S.K., Huang, Y. and Geng, J.X., ACS Appl. Mater. Interfaces, 2016, 8(18): 11711
26 Meng, D., Yang, S., Guo, L., Li, G., Ge, J., Huang, Y., Bielawski, C.W. and Geng, J., Chem. Commun., 2014, 50(92): 14345
27 Erb, T., Zhokhavets, U., Gobsch, G., Raleva, S., Stuhn, B., Schilinsky, P., Waldauf, C. and Brabec, C.J., Adv. Funct. Mater., 2005, 15(7): 1193

28 Kim, D.H., Park, Y.D., Jang, Y.S., Yang, H.C., Kim, Y.H., Han, J.I., Moon, D.G., Park, S.J., Chang, T.Y., Chang, C.W., Joo, M.K., Ryu, C.Y. and Cho, K.W., Adv. Funct. Mater., 2005, 15(1): 77
29 Chen, F.C., Lin, Y.K. and Ko, C.J., Appl. Phys. Lett., 2008, 92(2): 023307
30 Yang, F., Shtein, M. and Forrest, S.R., Nat. Mater., 2005, 4(1): 37
31 Yang, F., Shtein, M. and Forrest, S.R., J. Appl. Phys., 2005, 98(1): 014906
32 Chen, Y.Z., Wang, Z.B., Gong, Y.M., Huang, H.Y. and He, T.B., J. Phys. Chem. B, 2006, 110(4): 1647
33 Lee, J.I., Cho, S.H., Park, S.M., Kim, J.K., Kim, J.K., Yu, J.W., Kim, Y.C. and Russell, T.P., Nano Lett., 2008, 8(8): 2315
34 Wei, J.H., Coffey, D.C. and Ginger, D.S., J. Phys. Chem. B, 2006, 110(48): 24324
35 Park, L.Y., Munro, A.M. and Ginger, D.S., J. Am. Chem. Soc., 2008, 130(47): 15916
36 Yim, K.H., Zheng, Z.J., Friend, R.H., Huck, W.T.S. and Kim, J.S., Adv. Funct. Mater., 2008, 18(19): 2897
37 Im, S.G., Kim, B.S., Lee, L.H., Tenhaeff, W.E., Hammond, P.T. and Gleason, K.K., Macromol. Rapid Commun., 2008, 29(20): 1648
38 Khanduyeva, N., Senkovskyy, V., Beryozkina, T., Horecha, M., Stamm, M., Uhrich, C., Riede, M., Leo, K. and Kiriy, A., J. Am. Chem. Soc., 2009, 131(1): 153
39 Zhang, F.L., Nyberg, T. and Inganas, O., Nano Lett., 2002, 2(12): 1373
40 Li, D.W. and Guo, L.J., J. Phys. D: Appl. Phys., 2008, 41(10): 105115
41 Liu, J.S., Kadnikova, E.N., Liu, Y.X., McGehee, M.D. and Frechet, J.M.J., J. Am. Chem. Soc., 2004, 126(31): 9486
42 Bjerring, M., Nielsen, J.S., Nielsen, N.C. and Krebs, F.C., Macromolecules, 2007, 40(16): 6012
43 Bower, D.I., "An introduction to polymer physics", Cambridge University Press, Cambridge, 2002
44 Moons, E., J. Phys.: Condens. Matter, 2002, 14(47): 12235
45 Walheim, S., Ramstein, M. and Steiner, U., Langmuir, 1999, 15(14): 4828
46 Walheim, S., Boltau, M., Mlynek, J., Krausch, G. and Steiner, U., Macromolecules, 1997, 30(17): 4995
47 Yang, X.N., Loos, J., Veenstra, S.C., Verhees, W.J.H., Wienk, M.M., Kroon, J.M., Michels, M.A.J. and Janssen, R.A.J., Nano Lett., 2005, 5(4): 579
48 Kim, Y., Cook, S., Tuladhar, S.M., Choulis, S.A., Nelson, J., Durrant, J.R., Bradley, D.D.C., Giles, M., McCulloch, I., Ha, C.S. and Ree, M., Nat. Mater., 2006, 5(3): 197
49 Prosa, T.J., Winokur, M.J. and McCullough, R.D., Macromolecules, 1996, 29(10): 3654
50 Chai, L.G., Zhou, H.X., Sun, X.L., Li, H.H., Yan, S.K. and Yang, X.Q., Chinese J. Polym. Sci., 2016, 34(4): 513
51 Hou, W.P., Zhao, N.J., Meng, D., Tang, J., Zeng, Y., Wu, Y., Weng, Y.Z.W., Cheng, C.G., Xu, X.L., Li, Y., Zhang, J.P., Huang, Y., Bielawski, C.W. and Geng, J.X., ACS Nano, 2016, 10(5): 5189